Rate Limitations in the Lumazine Synthase Mechanism

Ya-Jun Zheng,* Paul V. Viitanen,† and Douglas B. Jordan‡·1

*E. I. DuPont Agricultural Products, Stine-Haskell Research Center, 1094 Elkton Road, P.O. Box 30,
Newark, Delaware 19714-0030; †E. I. DuPont Central Research and Development, Experimental
Station, Wilmington, Delaware 19880-0402; and ‡DuPont Pharmaceutical Company, Stine-Haskell
Research Center, 1094 Elkton Road, P.O. Box 30, Newark, Delaware 19714-0030

Lumazine synthase has a slow rate of catalysis: steady-state k_{cat} values for the *Escherichia coli, Magnaporthe grisea,* and spinach enzymes are 0.024, 0.052, and 0.023 s^{-1}, respectively, at pH 7.5 and 25°C. Following the formation of an imine connecting the two substrates 3,4-dihydroxy-2-butanone 4-phosphate and 4-ribitylamino-5-amino-2,6-dihydroxypyrimidine, there is a chemically difficult isomerization. Calculated estimates of the free energy barrier for the isomerization are equal to or greater than 15 kcal/mol at 25°C. Free energies calculated from the steady-state k_{cat} values at 25°C for the *E. coli, M. grisea,* and spinach enzymes are 19.7, 19.2, and 19.7 kcal/mol, respectively. The single-turnover rate (pre-steady state) at pH 7.5 and 25°C for the *M. grisea* enzyme is 140-fold greater than the steady-state rate and it has a free energy barrier of 16.3 kcal/mol. In the pre-steady state the *M. grisea* enzyme has a pK_a of 5.8, plausibly reporting the proposed general base of catalysis (His127). The *M. grisea* enzyme has an off rate of 0.37 s^{-1} for its product, 6,7-dimethyl-8-ribityllumazine, approximately 7-fold higher than k_{cat} and 20-fold lower than the single-turnover rate. The off rate for the product orthophosphate is about 1 s^{-1}. Thus, for the *M. grisea* enzyme at pH 7.5 and 25°C, product dissociation is significantly rate limiting to the steady-state rate of catalysis, whereas the isomerization step limits the single turnover rate. The spinach and *E. coli* enzymes display a significant lag in pre-steady state, suggesting that substrate association is significantly rate limiting for these catalysts. Temperature studies on the enzyme-catalyzed rates for the three enzymes indicate a dominating enthalpic term. © 2000 Academic Press

INTRODUCTION

Lumazine synthase (LS) catalyzes the penultimate step of riboflavin biosynthesis (*1–4*). A molecule of 3,4-dihydroxy-2-butanone 4-phosphate (DHBP) and one of 4-ribitylamino-5-amino-2,6-dihydroxypyrimidine (RAADP) are joined to form 6,7-dimethyl-8-(1′-D-ribityl)lumazine (DMRL) with the elimination of orthophosphate and two waters. Subsequently, riboflavin synthase (RS) catalyzes the dismutation of two molecules of DMRL to yield an equivalent of riboflavin and RAADP. LS can exist as a 60-mer in the form of an icosahedral capsid with or without a trimer of RS

---

[1] To whom correspondence and reprint requests should be addressed. Fax: (302) 366-5738. E-mail: doug.b.jordan@dupontpharma.com.

localized within (*5–11*) or as a pentamer lacking an association with RS (8,11,12), depending on its biological source and its condition. Association of the two terminal enzymes (LS and RS) of the pathway has been described as an instrument towards increasing catalytic efficiency (at low substrate concentrations) through a substrate-channeling mechanism (13). According to X-ray crystallographic studies, the quaternary structure of LS is determined by contacts of amino acid side chains that allow or disallow associations of pentamers (the minimal functional unit because of the organization of five active sites per pentamer) in forming a dodecrahedron of the pentamers (8,11,12). On the basis of its lack of functional counterparts in off-target organisms (e.g., humans and other animals) LS is a target for the design of inhibitors in antimicrobial programs (*14–16*).

In the crystal structures of LS, both the phosphate and the ribitylpyrimidine binding sites have been identified (*6,7,11*), allowing for a detailed mechanism to be proposed (*7,8*). Inspection of the proposed reaction path (Fig. 1) leads to the idea that the most difficult chemical step is in the isomerization of the double bond in the conversion of **3** to **4**. Unlike isomerization reactions catalyzed by numerous enzymes that employ active-site residues as general acids and bases, the isomerization of **3** to **4** is aprotic thus making it difficult for the enzyme to influence the rate. Thermal isomerization around a carbon–carbon double bond normally includes a large energy barrier; for instance, the barrier for a CHD=CHD isomerization is 65 kcal/mol (17). The activation energy for isomerization around a carbon–nitrogen double bond (as in transforming **3** to **4**) is expected to be smaller, but not insignificant. Indeed, the reported steady-state k_{cat} values for LS indicate a rather slow rate for catalysis (*3,4,10,11*). Here we examine the magnitude of the energy barrier for the isomerization step of the LS-catalyzed reaction (**3** to **4**) using a theoretical approach and compare the results to the rates of catalysis (steady-state and pre-steady state) observed for three LSs obtained from phylogenetically diverse sources.
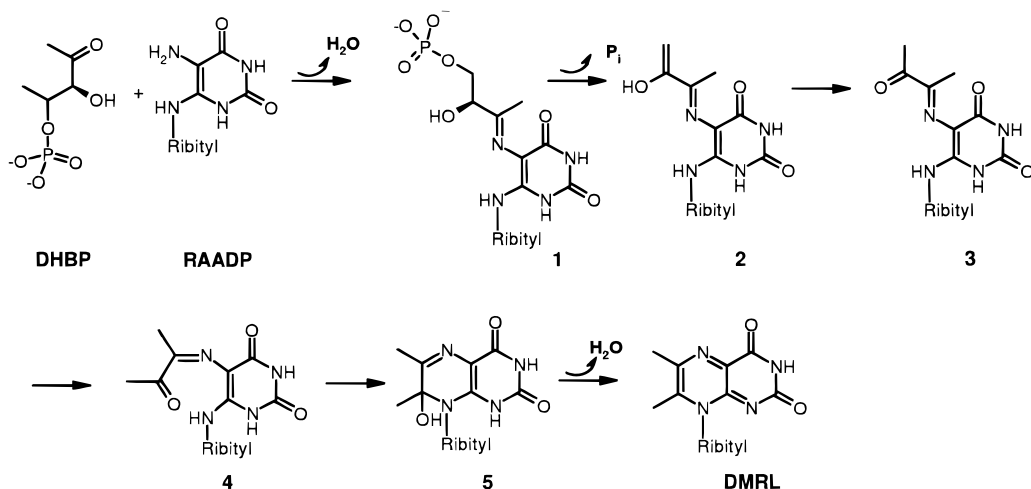

FIG. 1. The reaction path for the LS catalyzed reaction as modified from references 7 and 8.

MATERIALS AND METHODS

General. LS from *M. grisea* (11) and spinach (10) were cloned, expressed in *E. coli,* and purified as described. The *E. coli* LS was cloned and expressed in a similar fashion as reported (8); purification procedures were quite similar to those used for the *M. grisea* and spinach enzymes (10,11). Active site concentrations (one per protomer) were estimated from the 280-nm absorbencies of the proteins using extinction coefficients calculated through the Peptidesort program of the Genetics Computer Group (Wisconsin Package, Version 9, Genetics Computer Group, Madison, WI). LS substrates DHBP and RAADP were prepared as before (10). The product 6,7-dimethyl-8-ribityllumazine (DMRL) was synthesized from RAADP and 2,3-butadione (18). 2-amino-6-mercapto-7-methylpurine ribonucleoside and purine-nucleoside phosphorylase were from Molecular Probes (Eugene, Oregon). Unless indicated otherwise, linear and nonlinear least squares fittings were through the computer program RS1 (BBN Research Systems; Cambridge, MA).

Calculations. The geometry of each species was fully optimized unless otherwise indicated. For the ab initio calculations, the G2 theory (*19–21*) was used; for the semiempirical calculations, the AM1 method was employed (*22*).

Reactions. Steady-state parameters were determined at 25°C in 50 mM Tris–HCl, pH 7.5, and 1.0 mM dithiothreotol. The 1-ml reactions (60–300 s) included 1.0 mM RAADP when the rate limitation of varied DHBP concentrations was measured; the reactions included 1.0 mM DHBP when the rate limitation of varied RAADP concentrations was measured. Reactions were initiated with enzyme and the rates were recorded continuously on a HP 8542A spectrophotometer (Hewlett-Packard) by using a spectrophotometric method (10) that measures DMRL formation at 408 nm. Data were fitted to Eq. [1] for the determination of kinetic constants. k_{cat} is maximum velocity, K is the Michaelis constant, A is the varied substrate concentration, and v is the observed velocity.

$$v = \frac{k_{cat}}{1 + K/A} \qquad [1]$$

Steady-state measurements of k_{cat} at varied temperatures were conducted on a thermostated stopped-flow instrument (Applied Photophysics; Leatherhead, UK). Reactions (60 s) at varied temperatures were monitored for absorbency increases at 408 nm to detect product DMRL. The left syringe contained 1.0 mM DHBP in 100 mM sodium phosphate, pH 7.0; the right syringe contained 0.05 mM LS (*E. coli, M. grisea* or spinach LS), 1.5 mM RAADP, and 2.0 mM dithiothreitol in 100 mM sodium phosphate. The left and right syringes were mixed using equal volumes of each; the instrument dead time was estimated as 1.6 ms. Rate data were fitted to the instruments software for a burst followed by a steady state in determining the steady-state rate for the *M. grisea* enzyme and to a line for the *E. coli* and spinach enzymes.

Pre-steady state measurements at varied temperatures (25–40.5°C) and pH 7.5 were conducted on the thermostated stopped-flow instrument. The left syringe contained 0.15 mM RAADP, 1.5 mM DHBP, 1.0 mM dithiothreitol, and 200 mM Tris–HCl at pH 7.5. The right syringe contained 0.5 mM *E. coli, M. grisea,* or spinach LS. Absorbency increases were monitored at 408 nm to detect product DMRL. The single-turnover data for the *M. grisea* enzyme were fitted to a single exponential using the instruments software.

Pre-steady state measurements at varied pH (5.73 to 9.44) and 25°C were conducted on the thermostated stopped-flow instrument. The left syringe contained 0.15 mM RAADP, 1.5 mM DHBP, 1.0 mM dithiothreitol, and 200 mM Bis-Tris-Propane at varied pH. The right syringe contained 0.5 mM *M. grisea* LS in 50 mM Tris–HCl at pH 7.5. Absorbency increases were monitored at 408 nm to detect product DMRL. The single-turnover rates were fitted to a single exponential using the instruments software. Determined rates at varying pH values were fitted to Eq. [2], which describes the titration of two ionizable groups (one per side) causing a decrease on the basic side and the acidic side. *p* Represents the measured parameter, *P* is the pH independent value for the parameter, [H+] is the proton concentration, and K_a and K_b are the dissociation constants for the groups affecting catalysis.

$$p = \frac{P}{1 + K_b/[H+] + [H+]/K_a}$$ [2]

Pre-steady state measurements at 25°C and pH 7.5 to detect orthophosphate production and release from the *M. grisea* LS were conducted on the thermostated stopped-flow instrument using purine-nucleoside phosphorylase as the coupling enzyme (23). The left syringe contained 30 units/ml purine nucleoside phosphorylase, 1.0 mM DHBP, 1.0 mM 2-amino-6-mercapto-7-methylpurine ribonucleoside, and 50 mM Tris–HCl at pH 7.5. The right syringe contained 1.5 mM RAADP, 0.1 mM *M. grisea* LS, 1.0 mM dithiothreitol, and 50 mM Tris–HCl at pH 7.5. The reactions were monitored for absorbency at 360 nm. Rates were fitted to a burst followed by a steady state using the instruments software.

Binding rates of DMRL to the *M. grisea* LS were determined using the thermostated stopped-flow instrument at 25°C. The left syringe contained 200 mM Tris–HCl, pH 7.5, and varying concentrations of DMRL (0.0675 to 2.0 μM). The right syringe contained 0.4 μM *M. grisea* LS in 200 mM Tris–HCl, pH 7.5. The reactions were monitored by following the quenching of DMRL fluorescence upon binding to the enzyme (nearly complete quenching when bound). Excitation was at 390 nm and emission was through a 450-nm-long pass filter.

RESULTS AND DISCUSSION

Isomerization about a C=N double bond can occur via either an in-plane inversion at the nitrogen center or an out-of-plane rotation about the double bond. The in-plane inversion does not require the double bond to be broken, while the out-of-plane rotation does. Therefore, the former pathway is expected to be preferred. Both semiempirical and high level ab initio molecular orbital methods are capable of providing an estimations of the inversion barrier. Since the compounds involved (**3** and **4**) are rather large, high level ab initio molecular orbital method cannot be applied directly. The semiempirical method can be applied to a very large system as in this case; however, these methods may not be accurate enough to give a definitive answer. Therefore, we decided to calibrate the semiempirical AM1 method on a model compound where a high level ab initio molecular orbital method can be applied. The comparison between the AM1 and high level ab initio results provides us with information about the uncertainty in the AM1 result. First of all, we carried out both AM1 and G2 calculations on compound **6** (Fig. 2).